# Match-up database Analyses Report

SMOS SSS L4 v1 - Monthly (CMEMS-CNR)

Moorings

Global Ocean

*prepared by the Pi-MEP Consortium*

June 15, 2022

# Contents

# List of Figures

# Acronym

| | |
|---|---|
| Aquarius | NASA/CONAE Salinity mission |
| ASCAT | Advanced Scatterometer |
| ATBD | Algorithm Theoretical Baseline Document |
| BLT | Barrier Layer Thickness |
| CMORPH | CPC MORPHing technique (precipitation analyses) |
| CPC | Climate Prediction Center |
| CTD | Instrument used to measure the conductivity, temperature, and pressure of seawater |
| DM | Delayed Mode |
| EO | Earth Observation |
| ESA | European Space Agency |
| FTP | File Transfer Protocol |
| GOSUD | Global Ocean Surface Underway Data |
| GTMBA | The Global Tropical Moored Buoy Array |
| Ifremer | Institut français de recherche pour l'exploitation de la mer |
| IPEV | Institut polaire français Paul-Émile Victor |
| IQR | Interquartile range |
| ISAS | *In Situ* Analysis System |
| Kurt | Kurtosis (fourth central moment divided by fourth power of the standard deviation) |
| L2 | Level 2 |
| LEGOS | Laboratoire d'Etudes en Géophysique et Océanographie Spatiales |
| LOCEAN | Laboratoire d'Océanographie et du Climat : Expérimentations et Approches Numériques |
| LOPS | Laboratoire d'Océanographie Physique et Spatiale |
| MDB | Match-up Data Base |
| MEOP | Marine Mammals Exploring the Oceans Pole to Pole |
| MLD | Mixed Layer Depth |
| NCEI | National Centers for Environmental Information |
| NRT | Near Real Time |
| NTAS | Northwest Tropical Atlantic Station |
| OI | Optimal interpolation |
| Pi-MEP | Pilot-Mission Exploitation Platform |
| PIRATA | Prediction and Researched Moored Array in the Atlantic |
| QC | Quality control |
| $R_{sat}$ | Spatial resolution of the satellite SSS product |
| RAMA | Research Moored Array for African-Asian-Australian Monsoon Analysis and Prediction |
| $r^2$ | Square of the Pearson correlation coefficient |
| RMS | Root mean square |
| RR | Rain rate |
| SAMOS | Shipboard Automated Meteorological and Oceanographic System |
| Skew | Skewness (third central moment divided by the cube of the standard deviation) |
| SMAP | Soil Moisture Active Passive (NASA mission) |
| SMOS | Soil Moisture and Ocean Salinity (ESA mission) |
| SPURS | Salinity Processes in the Upper Ocean Regional Study |
| SSS | Sea Surface Salinity |
| $SSS_{insitu}$ | *In situ* SSS data considered for the match-up |

| | |
|---|---|
| $SSS_{SAT}$ | Satellite SSS product considered for the match-up |
| $\Delta SSS$ | Difference between satellite and *in situ* SSS at colocalized point ($\Delta SSS = SSS_{SAT}$- $SSS_{insitu}$) |
| SST | Sea Surface Temperature |
| Std | Standard deviation |
| Std$^\star$ | Robust Standard deviation = median(abs(x-median (x)))/0.67 (less affected by outliers than Std) |
| Stratus | Surface buoy located in the eastern tropical Pacific |
| Survostral | SURVeillance de l'Océan AuSTRAL (Monitoring the Southern Ocean) |
| TAO | Tropical Atmosphere Ocean |
| TSG | ThermoSalinoGraph |
| WHOI | Woods Hole Oceanographic Institution |
| WHOTS | WHOI Hawaii Ocean Time-series Station |
| WOA | World Ocean Atlas |

# 1   Overview

In this report, we present systematic analyses of the Match-up DataBase (MDB) files generated by the Pi-MEP platform and merged into a single file available here for the below pair of Satellite/*in situ* SSS data:

- SSS satellite product ($SSS_{SAT}$): SMOS SSS L4 v1 - Monthly (CMEMS-CNR)

- *In situ* dataset ($SSS_{Insitu}$): Moorings (download the corresponding *in situ* report here)

In the following, $\Delta SSS = SSS_{SAT} - SSS_{Insitu}$ denotes the difference between the satellite and *in situ* SSS at the colocalized points that form the MDB.

This report presents successively:

The MDB file DataSets (Section 2)

- A short description of the satellite SSS product considered in the match-up (2.1)

- A short description of the *in situ* SSS dataset considered in the match-up (2.2)

- A short description of the auxiliary geophysical datasets co-localized with SSS pairs (2.3)

- An overview of how the Match-ups were evaluated (2.4)

- An overview of the MDB characteristics for the particular *in situ*/satellite pairs (**??**)

The major results of the MDB file Analyses (Section 3)

- Time-series of mooring and satellite salinity (3.1)

- Time-series of mooring and models/*in situ* analyses salinity (3.2)

- Power spectrum of SSS for each mooring (3.3)

- Average of all mooring power spectra (3.4)

All analyses are conducted over the full satellite SSS product period. Original figures appearing in this report can be downloaded here as PNG files.

# 2 The MDB file datasets

## 2.1 Satellite SSS product

### 2.1.1 SMOS SSS L4 v1 - Monthly (CMEMS-CNR)

Global gap-free Level-4 (L4) monthly analyses of Sea Surface Salinity (SSS) obtained through a multivariate optimal interpolation algorithm that combines Soil Moisture Ocean Salinity (SMOS) satellite images and in situ salinity measurements with satellite SST information. The product was developed by the Consiglio Nazionale delle Ricerche (CNR).

Table 1: Satellite SSS product characteristics

| SMOS SSS L4 v1 - Monthly (CMEMS-CNR) | |
|---|---|
| Spatial resolution | 0.25° |
| Temporal resolution | Monthly |
| Temporal coverage | From 2011-01-24 to present |
| Spatial coverage | LGlobal [-180 180 -90 90] |
| Data Provider | CMEMS |
| Institution | Consiglio Nazionale delle Ricerche (CNR) |
| Version | 1 |
| Quality report | CMEMS-MOB-QUID-015-013.pdf |
| DOI | https://doi.org/10.48670/moi-00051 |
| References | Droghei et al. (2016); Nardelli et al. (2016); Droghei et al. (2018) |

## 2.2 *In situ* SSS dataset

The Pi-MEP collects data from the Global Tropical Moored Buoy Array (GTMBA), a multi-national effort to provide data in real-time for climate research and forecasting. Major components include the TAO/TRITON array in the Pacific, PIRATA in the Atlantic, and RAMA in the Indian Ocean. Data collected within TAO/TRITON, PIRATA and RAMA come primarily from ATLAS and TRITON moorings. These two mooring systems are functionally equivalent in terms of sensors, sample rates, and data quality. The data are directly downloaded from ftp.pmel.noaa.gov every day and stored in the Pi-MEP. Only salinity data measured at 1 or 1.5 meter depth with standard (pre-deployment calibration applied) and highest quality (pre/post calibration in agreement) are considered. A careful filtering of suspiciously erroneous mooring salinity data when compared with all satellite data has also been performed (cf. presentation). The Pi-MEP project acknowledges the GTMBA Project Office of NOAA/PMEL for providing the data. Data from the Ocean Station PAPA are also added to the Pi-MEP *in situ* database.

From the Upper Ocean Processes Group at Woods Hole Oceanographic Institution (WHOI), several moorings data are also included in the Pi-MEP. Namely, delayed mode surface mooring salinity records under the stratus cloud deck in the eastern tropical Pacific (Stratus), in the trade wind region of the northwest tropical Atlantic (NTAS), 100 km north of Oahu at the WHOI Hawaii Ocean Time-series Site (WHOTS), in the salinity maximum region of the subtropical North Atlantic (SPURS-1) and in the Pacific intertropical convergence zone (SPURS-2).

## 2.3  Auxiliary geophysical datasets

Additional EO datasets are used to characterize the geophysical conditions at the *in situ*/satellite SSS pair measurement locations and time, and 10 days prior to the measurements, to get an estimate of the geophysical concomitant condition and history. As discussed in Boutin et al. (2016), the presence of vertical gradients in, and horizontal variability of, sea surface salinity indeed complicates comparison of satellite and *in situ* measurements. The additional EO data are used here to get a first estimates of conditions for which L-band satellite SSS measured in the first centimeters of the upper ocean within a 50-150 km diameter footprint might differ from pointwise *in situ* measurements performed in general between 10 and 5 m depth below the surface. The spatio-temporal variability of SSS within a satellite footprint (50–150 km) is a major issue for satellite SSS validation in the vicinity of river plumes, frontal zones, and significant precipitation areas, among others. Rainfall can in some cases produce vertical salinity gradients exceeding 1 pss m$^{-1}$; consequently, it is recommended that satellite and *in situ* SSS measurements less than 3–6 h after rain events should be considered with care when used in satellite calibration/validation analyses. To identify such situation, the Pi-MEP platform is first using CMORPH products to characterize the local value and history of rain rate and ASCAT gridded data are used to characterize the local surface wind speed and history. For validation purpose, the ISAS monthly SSS *in situ* analysed fields at 5 m depth are collocated and compared with the satellite SSS products. The use of ISAS is motivated by the fact that it is used in the SMOS L2 official validation protocol in which systematic comparisons of SMOS L2 retrieved SSS with ISAS are done. In complement to ISAS, monthly std climatological fields from the World Ocean Atlas (WOA13) at the match-up pairs location and date are also used to have an a priori information of the local SSS variability.

### 2.3.1  ISAS

The In Situ Analysis System (ISAS), as described in Gaillard et al. (2016) is a data based re-analysis of temperature and salinity fields over the global ocean 70°N–70°S on a 1/2° grid. It was initially designed to synthesize the temperature and salinity profiles collected by the Argo program. It has been later extended to accommodate all type of vertical profile as well as time series. ISAS gridded fields are entirely based on *in situ* measurements. The methodology and configuration have been conceived to preserve as much as possible the data information content and resolution. ISAS is developed and run in a research laboratory (LOPS) in close collaboration with Coriolis, one of Argo Global Data Assembly Center and unique data provider for the Mercator operational oceanography system. In Pi-MEP, the products used are the IN-SITU_GLO_TS_OA_REP_OBSERVATIONS_013_002_b for the period 2010 to 2019 and the IN-SITU_GLO_TS_OA_NRT_OBSERVATIONS_013_002_a for the Near-Real Time (2020-2021) derived at the Coriolis data center and provided by the Copernicus Marine Environment Monitoring Service (CMEMS). The major contribution to the data set is from Argo array of profiling floats, reaching an approximate resolution of one profile every 10-days and every 3-degrees over the satellite SSS period (http://www.umr-lops.fr/SNO-Argo/Products/ISAS-T-S-fields/); in this version SSS from ship of opportunity thermosalinographs are not used, so that we can consider SMOS SSS validation using these measurements independent of ISAS. The ISAS optimal interpolation involves a structure function modeled as the sum of two Gaussian functions, each associated with specific time and space scales, resulting in a smoothing over typically 3 degrees. The smallest scale which can be retrieved with ISAS analysis is not smaller than 300–500 km (Kolodziejczyk et al. (2015)). For validation purpose, the ISAS monthly SSS fields at 5 m depth are collocated and compared with the satellite SSS products and included in the Pi-MEP Match-up files. In addition, the "percentage of variance" fields (PCTVAR) contained in the

ISAS analyses provide information on the local variability of *in situ* SSS measurements within $1/2°\times1/2°$ boxes.

### 2.3.2 Mercator

The Operational Mercator global ocean analysis and forecast system at 1/12 degree is providing 10 days of 3D global ocean forecasts updated daily. The time series start on December 27, 2006 and is aggregated in time in order to reach a two full year's time series sliding window.This product includes daily and monthly mean files of temperature, salinity, currents, sea level, mixed layer depth and ice parameters from the top to the bottom over the global ocean. It also includes hourly mean surface fields for sea level height, temperature and currents. The global ocean output files are displayed with a 1/12 degree horizontal resolution with regular longitude/latitude equirectangular projection. 50 vertical levels are ranging from 0 to 5500 meters.

The high resolution global analysis and forecasting system PSY4V3R1 uses version 3.1 of NEMO ocean model (Madec (2008)). The physical configuration is based on the tripolar ORCA grid type (Madec and Imbard (1996)) with a horizontal resolution of 9 km at the equator, 7 km at Cape Hatteras (mid-latitudes) and 2 km toward the Ross and Weddell seas. The 50-level vertical discretization retained for this system has 1 m resolution at the surface decreasing to 450 m at the bottom, and 22 levels within the upper 100 m. The bathymetry used in the system is a combination of interpolated ETOPO1 (Amante and Eakins (2009)) and GEBCO8 (Becker et al. (2009)) databases. ETOPO1 datasets are used in regions deeper than 300 m and GEBCO8 is used in regions shallower than 200 m with a linear interpolation in the 200-300 m layer. The atmospheric fields forcing the ocean model are taken from the ECMWF (European Centre for Medium-Range Weather Forecasts) Integrated Forecast System. A 3 h sampling is used to reproduce the diurnal cycle. The system does not include tides. "Partial cells" parametrization (Adcroft et al. (1997)) is chosen for a better representation of the topographic floor (Bernard et al. (2006)) and the momentum advection term is computed with the energy and enstrophy conserving scheme proposed by Arakawa and Lamb (1981). The advection of the tracers (temperature and salinity) is computed with a total variance diminishing (TVD) advection scheme (Lévy et al., 2001; Cravatte et al. (2007)). The high frequency gravity waves are filtered out by a free surface (Roullet and Madec (2000)). A laplacian lateral isopycnal diffusion on tracers and a horizontal biharmonic viscosity for momentum are used. In addition, the vertical mixing is parametrized according to a turbulent closure model (order 1.5) adapted by Blanke and Delecluse (1993), the lateral friction condition is a partial-slip condition with a regionalisation of ano-slip condition (over the Mediterranean Sea) and the Elastic-Viscous-Plastic rheology formulation for the LIM2 ice model (hereafter called LIM2_EVP, Fichefet and Maqueda (1997)) has been activated (Hunke and Dukowicz (1997)). Instead of being constant, the depth of light extinction is separated in Red-Green-Blue bands depending on the chlorophyll data distribution from mean monthly SeaWIFS climatology. Altimeter data, *in situ* temperature and salinity vertical profiles and satellite sea surface temperature are jointly assimilated to estimate the initial conditions for numerical ocean forecasting.Moreover, satellite sea ice concentration is now assimilated in the PSY4V3R1 system in a monovariate/monodata mode.

The Pi-MEP uses daily salinity fields at the surface (GLOBAL_ANALYSIS_FORECAST_PHY_001_024) provided by the Copernicus Marine environment monitoring service (CMEMS) and freely available here. For more information, please refer to the user manual (CMEMS-GLO-PUM-001-024.pdf) and quality information document (CMEMS-GLO-QUID-001-024.pdf)

### 2.3.3 Hycom

Pi-MEP uses daily HYCOM+NCODA Global 1/12° Analysis product interpolates on a uniform 0.08 degree lat/lon grid between 80.48S and 80.48N (GLBu0.08). HYCOM is a data-assimilative hybrid isopycnal-sigma-pressure (generalized) coordinate ocean model (called HYbrid Coordinate Ocean Model). It uses the Navy Coupled Ocean Data Assimilation (NCODA) system (Cummings (2005), Cummings and Smedstad (2013)) for data assimilation. NCODA uses the model forecast as a first guess in a 3D variational scheme and assimilates available satellite altimeter observations (along track obtained via the NAVOCEANO Altimeter Data Fusion Center) satellite and *in situ* Sea Surface Temperature (SST) as well as available *in situ* vertical temperature and salinity profiles from XBTs, ARGO floats and moored buoys. MODAS synthetics are used for downward projection of surface information (Fox et al. (2002)).

### 2.3.4 ECCO

Version 4 Release 3 (V4r3), covering the period 1992-2015, represents the latest ocean state estimate of the Consortium for Estimating the Circulation and Climate of the Ocean (ECCO) (Wunsch et al. (2009); Wunsch and Heimbach (2013)) that synthesizes nearly all modern observations with an ocean circulation model (MITgcm, originally described by Marshall et al. (1997)) into coherent, physically consistent descriptions of the ocean's time-evolving state covering the era of satellite altimetry. Among its characteristics, Version 4 (Forget et al. (2015a)) is the first multidecadal ECCO estimate that is truly global, including the Arctic Ocean. Unlike previous versions, the model uses a nonlinear free surface formulation and real freshwater flux boundary condition, permitting a more accurate simulation of sea level change. In addition to estimating forcing and initial conditions as done in earlier analyses, the Version 4 estimate also adjusts the model's mixing parameters that enables an improved fit to observations (Forget et al. (2015b)). The Version 4 synthesis also incorporates a diffusion operator in evaluating model-data misfits (Forget and Ponte (2015)) and controls (Weaver and Courtier (2001)), accounting for some of the spatial correlation that exist among these elements. The Release 3 edition includes improvements in time-period (1992-2015), model (e.g., sea-ice), observations (e.g., GRACE, Aquarius), and constraints (e.g., correlated errors).

## 2.4 Overview of the Match-ups generation method

The match-up production is basically a three steps process:

1. preparation of the input *in situ* and satellite data, and,

2. co-localization of satellite products with *in situ* SSS measurements.

3. co-localization of the *in situ*/satellite pair with auxiliary information.

In the following, we successively detail the approaches taken for these different steps.

### 2.4.1 *In Situ*/Satellite data filtering

The first step consists in filtering Moorings *in situ* dataset using the quality flags as described in 2.2 so that only valid salinity data remains in the produced match-ups.

For high-temporal resolution *in situ* SSS measurements such as moorings, an additional temporal-filtering step is performed on the *in situ* data that will be in fine compared to the satellite SSS products. A running median filtered is applied with a window width of $D$, the

period over which the composite product was built. Both the original and the filtered data are finally stored in the MDB files.

Only for satellite L2 SSS data, a third step consist in filtering spurious data using the flags and associated recommendation as provided by the official data centers and described in 2.1.

### 2.4.2  *In Situ*/Satellite Co-localization

In this step, each SSS satellite acquisition is co-localized with the filtered *in situ* measurements. The method used for co-localization differ if the satellite SSS is a swath product (so-called Level 2-types) or a time-space composite product (so-called Level 3/level 4-types).

- For L2 SSS swath data :

  If $R_{sat}$ is the spatial resolution of the satellite swath SSS product, for each *in situ* data sample collected in the Pi-MEP database, the platform searches for all satellite SSS data found at grid nodes located within a radius of $R_{sat}/2$ from the *in situ* data location and acquired with a time-lag from the *in situ* measurement date that is less or equal than $\pm 12$ hours. If several satellite SSS samples are found to meet these criteria, the final satellite SSS match-up point is selected to be the closest in time from the *in situ* data measurement date. The final spatial and temporal lags between the *in situ* and satellite data are stored in the MDB files.

- For L3 and L4 composite SSS products :

  If $R_{sat}$ is the spatial resolution of the composite satellite SSS product and $D$ the period over which the composite product was built (e.g., periods of 1, 7, 8, 9, 10, 18 days, 1 month, etc..) with central time $t_o$, for each *in situ* data sample collected in the Pi-MEP database during period $D$, the platform searches for all satellite SSS data of the composite product found at grid nodes located within a radius of $R_{sat}/2$ from the *in situ* data location. If several satellite SSS product samples are found to meet these criteria, the final satellite SSS match-up point is chosen to be the composite SSS with central time $t_o$ which is the closest in time from the *in situ* data measurement date. The final spatial and temporal lags between the *in situ* and satellite data are stored in the MDB files.

### 2.4.3  MDB pair Co-localization with auxiliary data and complementary information

MDB data consist of satellite and *in situ* SSS pairs but also of other auxiliary SSS sources which are included in the final match-up files. The collocation is done for each *in situ* SSS measurement contained in the match-up files as follows:

For the given day of the *in situ* data, we select the Hycom and Mercator SSS field of the same day than $t_{insitu}$ found at the closest grid node from the *in situ* data location.

For the given month of the *in situ* data, we select the ISAS and ECCO fields for the same month and take the SSS analysis found at the closest grid node from the *in situ* measurement.

The distance from the *in situ* SSS data location to the nearest coast is evaluated and provided in km. We use a distance-to-coast map at $1/4°$ resolution where small islands have been removed.

The resulting match-ups files are serialized as NetCDF-4 files and merged into a single file available here whose structure is described on section 2.4.4.

### 2.4.4  Content of the Match-Up NetCDF files

netcdf pimep-mdb-final-_smos-l4-cmems-cnr-v1-1m_mooring_v01 {
dimensions:

9

```
        TIME_SAT = UNLIMITED ; // (1 currently)
        TIME_MOORING = 80473 ;
        N_moorings = 140 ;
        STRING17 = 17 ;

    variables:
double DATE_Satellite_product(TIME_Sat) ;
        DATE_Satellite_product:long_name = "Central time of satellite SSS file" ;
        DATE_Satellite_product:units = "days since 1990-01-01 00:00:00" ;
        DATE_Satellite_product:standard_name = "time" ;
float LATITUDE_Satellite_product(TIME_MOORING) ;
        LATITUDE_Satellite_product:long_name = "Satellite product latitude at mooring location"
;
        LATITUDE_Satellite_product:units = "degrees_north" ;
        LATITUDE_Satellite_product:valid_min = -90. ;
        LATITUDE_Satellite_product:valid_max = 90. ;
        LATITUDE_Satellite_product:standard_name = "latitude" ;
        LATITUDE_Satellite_product:_FillValue = -999.f ;
float LONGITUDE_Satellite_product(TIME_MOORING) ;
        LONGITUDE_Satellite_product:long_name = "Satellite product longitude at mooring lo-
cation" ;
        LONGITUDE_Satellite_product:units = "degrees_east" ;
        LONGITUDE_Satellite_product:valid_min = -180. ;
        LONGITUDE_Satellite_product:valid_max = 180. ;
        LONGITUDE_Satellite_product:standard_name = "longitude" ;
        LONGITUDE_Satellite_product:_FillValue = -999.f ;
float SSS_Satellite_product(TIME_MOORING) ;
        SSS_Satellite_product:long_name = "Satellite product SSS at mooring location" ;
        SSS_Satellite_product:units = "1" ;
        SSS_Satellite_product:salinity_scale = "Practical Salinity Scale(PSS-78)" ;
        SSS_Satellite_product:standard_name = "sea_surface_salinity" ;
        SSS_Satellite_product:_FillValue = -999.f ;
float SST_Satellite_product(TIME_MOORING) ;
        SST_Satellite_product:long_name = "Satellite product SST at mooring location" ;
        SST_Satellite_product:units = "degree Celsius" ;
        SST_Satellite_product:standard_name = "sea_surface_temperature" ;
        SST_Satellite_product:_FillValue = -999.f ;
float Spatial_lags(TIME_MOORING) ;
        Spatial_lags:long_name = "Spatial lag between mooring location and satellite SSS product
pixel center" ;
        Spatial_lags:units = "km" ;
        Spatial_lags:_FillValue = -999.f ;
double DATE_MOORING(TIME_MOORING) ;
        DATE_MOORING:long_name = "Mooring time" ;
        DATE_MOORING:units = "days since 1990-01-01 00:00:00" ;
        DATE_MOORING:standard_name = "time" ;
        DATE_MOORING:_FillValue = -999.f ;
float LATITUDE_MOORING(TIME_MOORING) ;
        LATITUDE_MOORING:long_name = "Mooring latitude" ;
```

        LATITUDE_MOORING:units = "degrees_north" ;
        LATITUDE_DRIFTER:valid_min = -90. ;
        LATITUDE_MOORING:valid_max = 90. ;
        LATITUDE_MOORING:standard_name = "latitude" ;
        LATITUDE_MOORING:_FillValue = -999.f ;
float LONGITUDE_MOORING(TIME_MOORING) ;
        LONGITUDE_MOORING:long_name = "Mooring longitude" ;
        LONGITUDE_MOORING:units = "degrees_east" ;
        LONGITUDE_MOORING:valid_min = -180. ;
        LONGITUDE_MOORING:valid_max = 180. ;
        LONGITUDE_MOORING:standard_name = "longitude" ;
        LONGITUDE_MOORING:_FillValue = -999.f ;
float SSS_MOORING(TIME_MOORING, N_moorings) ;
        SSS_MOORING:long_name = "Mooring SSS" ;
        SSS_MOORING:units = "1" ;
        SSS_MOORING:salinity_scale = "Practical Salinity Scale(PSS-78)" ;
        SSS_MOORING:standard_name = "sea_water_salinity" ;
        SSS_MOORING:_FillValue = -999.f ;
float SSS_MOORING_FILTERED(TIME_MOORING, N_moorings) ;
        SSS_MOORING_FILTERED:long_name = "Median filtered mooring SSS at satellite tem-
poral resolution" ;
        SSS_MOORING_FILTERED:units = "1" ;
        SSS_MOORING_FILTERED:salinity_scale = "Practical Salinity Scale(PSS-78)" ;
        SSS_MOORING_FILTERED:standard_name = "sea_water_salinity" ;
        SSS_MOORING_FILTERED:_FillValue = -999.f ;
float SSS_QC_MOORING(TIME_MOORING, N_moorings) ;
        SSS_QC_MOORING:long_name = "Mooring SSS Quality indices (Highest Quality=1, De-
fault Quality=2, Adjusted Data=3, Lower Quality=4)" ;
        SSS_QC_MOORING:units = "1 ;
        SSS_QC_MOORING:_FillValue = -999.f ;
float DEPTH_MOORING(N_moorings) ;
        DEPTH_MOORING:long_name = "Mooring SSS Depth" ;
        DEPTH_MOORING:units = "m" ;
        DEPTH_MOORING:_FillValue = -999.f ;
char NAME_MOORING(N_moorings) ;
        NAME_MOORING:long_name = "Mooring name" ;
float DISTANCE_TO_COAST_MOORING(TIME_MOORING) ;
        DISTANCE_TO_COAST_MOORING:long_name = "Distance to coasts at mooring loca-
tion" ;
        DISTANCE_TO_COAST_MOORING:units = "km" ;
        DISTANCE_TO_COAST_MOORING:_FillValue = -999.f ;
float SSS_HYCOM(TIME_MOORING, N_moorings) ;
        SSS_HYCOM:long_name = "HYCOM SSS (depth=0m) from GLBu0.08 at mooring loca-
tion" ;
        SSS_HYCOM:units = "1" ;
        SSS_HYCOM:salinity_scale = "Practical Salinity Scale(PSS-78)" ;
        SSS_HYCOM:standard_name = "sea_water_salinity" ;
        SSS_HYCOM:_FillValue = -999.f ;

```
    float SSS_MERCATOR(TIME_MOORING, N_moorings) ;
      SSS_MERCATOR:long_name = "MERCATOR SSS (depth=0.5m) from CMEMS (GLOBAL_ANALYSIS_FOREC
at mooring location" ;
      SSS_MERCATOR:units = "1" ;
      SSS_MERCATOR:salinity_scale = "Practical Salinity Scale(PSS-78)" ;
      SSS_MERCATOR:standard_name = "sea_water_salinity" ;
      SSS_MERCATOR:_FillValue = -999.f ;

    float SSS_ISAS(TIME_MOORING, N_moorings) ;
      SSS_ISAS:long_name = "ISAS SSS (5m depth) from CMEMS (INSITU_GLO_TS_OA_NRT_OBSERVATIONS_013
at mooring location" ;
      SSS_ISAS:units = "1" ;
      SSS_ISAS:salinity_scale = "Practical Salinity Scale(PSS-78)" ;
      SSS_ISAS:standard_name = "sea_water_salinity" ;
      SSS_ISAS:_FillValue = -999.f ;

    float SSS_ECCO(TIME_MOORING, N_moorings) ;
      SSS_ECCO:long_name = "ECCO (v4r3) SSS (5m depth) at mooring location" ;
      SSS_ECCO:units = "1" ;
      SSS_ECCO:salinity_scale = "Practical Salinity Scale(PSS-78)" ;
      SSS_ECCO:standard_name = "sea_water_salinity" ;
      SSS_ECCO:_FillValue = -999.f ;

    // global attributes:
      :Conventions = "CF-1.6" ;
      :title = "Moorings Match-Up Database" ;
      :Satellite_product_name = "SMOS SSS L4 v1 - Monthly (CMEMS-CNR)" ;
      :Satellite_product_spatial_resolution = "0.25 deg" ;
      :Match-Up_spatial_window_radius_in_km = 13.5;
      :Match-Up_temporal_window_radius_in_days = 15;
      :start_time = "20100114T000005Z" ;
      :stop_time = "20190308T000000Z" ;
      :northernmost_latitude = 24.58112f ;
      :sourthenmost_latitude = -25f ;
      :westernmost_longitude = -179.219f ;
      :easternmost_longitude = 179.199f ;
      :geospatial_lat_units = "degrees north" ;
      :geospatial_lat_resolution = "0.25 deg" ;
      :geospatial_lon_units = "degrees east" ;
      :geospatial_lon_resolution = "0.25 deg" ;
      :institution = "ESA-IFREMER-ODL-OCEANSCOPE" ;
      :project_name = "SMOS Pilot-Mission Exploitation Platform (Pi-MEP) for salinity" ;
      :project_url = "https://www.salinity-pimep.org" ;
      :license = "Pi-MEP data use is free and open" ;
      :product_version = "1.0" ;
      :keywords = "Oceans > Ocean Salinity > Sea Surface Salinity" ;
      :acknowledgment = "Please acknowledge the use of these data with the following statement:
These data were provided by SMOS Pilot-Mission Exploitation Platform (Pi-MEP) for salinity"
;
```

:In_situ_data_source = "ftp://ftp.pmel.noaa.gov/cdf/fields/ and http://uop.whoi.
edu/currentprojects/";        :references = "https://www.salinity-pimep.org" ;
    :history = "Processed on 2018-04-18 using MDB_generator" ;
    :date_created = "2019-09-18 17:09:30" ;
}

# 3  MDB file Analyses

## 3.1  Time-series of mooring and satellite salinity

In Figure 1, time series of SSS from Moorings (black curve) and SMOS SSS L4 v1 - Monthly
(CMEMS-CNR) (red curve) satellite SSS product at each mooring location is shown. To switch
from a mooring location to another, you can play with the arrows between the plot and the
caption.

Figure 1: Time series of SSS from Moorings and SMOS SSS L4 v1 - Monthly (CMEMS-CNR)
satellite SSS product.

## 3.2  Time-series of mooring and models/*in situ* analyses salinity

In Figure 2, time series of SSS from Moorings (black curve), models (Hycom in cyan, Mercator
in blue and ECCO in magenta) and in situ analyses ISAS (red curve) at each mooring location
is shown. To switch from a mooring location to another, you can play with the arrows between
the plot and the caption.

Figure 2: Time series of SSS from Moorings, models (Hycom, Mercator, ECCO) and monthly Argo *in situ* analyses (ISAS).

## 3.3   Power spectrum of SSS for each mooring

In Figure 3, we estimate the frequency averaged power spectrum with geophysical normalization after trend has been removed, using a Blackman-Harris window for each individual mooring/satellite match-up time series. Numerical values can be downloaded as a NetCDF file here.

Figure 3: Power spectrum of SSS from Moorings (black), SMOS SSS L4 v1 - Monthly (CMEMS-CNR) satellite SSS product (red), ISAS (blue) and Mercator (pink) for each individual mooring/satellite match-up time series.

## 3.4 Average of all mooring power spectra

In Figure 4, we average all power spectra calculated previously for mooring (black), satellite (red), ISAS (blue) and Mercator (dashed magenta) time series.
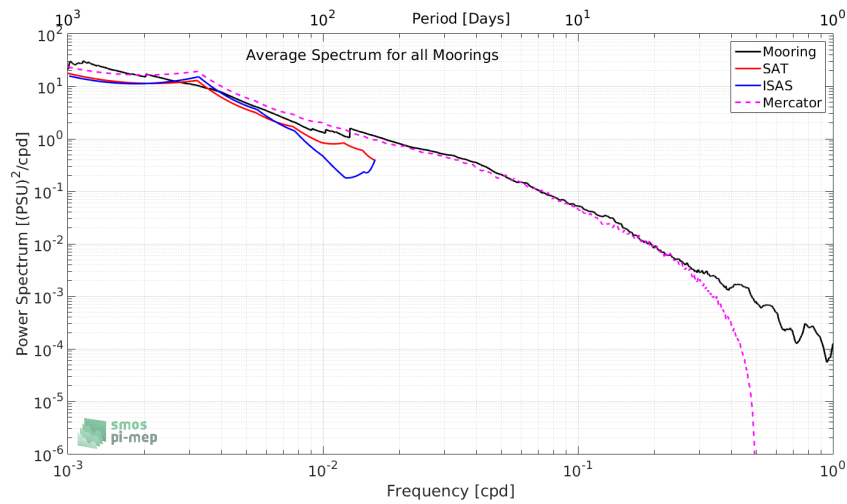


Figure 4: Average of all mooring (black), satellite (red), ISAS (blue) and Mercator (dashed magenta) SSS power spectra.

# 4 Summary

Table 1 shows the mean, median, standard deviation (Std), root mean square (RMS), interquartile range (IQR), correlation coefficient ($r^2$) and robust standard deviation ($Std^\star$) of the match-up differences $\Delta$SSS (Satellite - *in situ$_{filtered}$*) between SMOS SSS L4 v1 - Monthly (CMEMS-CNR) SSS satellite product and filtered Moorings for the full satellite product period. Same statistical values are also shown for different $\Delta$SSS: (Satellite - *in situ*), (Satellite - ISAS), (Satellite - Mercator), (ISAS - Mooring), (Mercator - Mooring) and (ISAS - Mercator).

**Table 1: Statistics of $\Delta$SSS**

| Condition | # | Median | Mean | Std | RMS | IQR | $r^2$ | $Std^\star$ |
|---|---|---|---|---|---|---|---|---|
| Satellite - Mooring (filtered) | 8745 | 0.00 | 0.00 | 0.22 | 0.22 | 0.20 | 0.95 | 0.15 |
| Satellite - Mooring | 9305 | 0.00 | 0.01 | 0.25 | 0.25 | 0.23 | 0.93 | 0.17 |
| Satellite - ISAS | 22344 | 0.00 | -0.01 | 0.14 | 0.14 | 0.12 | 0.98 | 0.09 |
| Satellite - Mercator | 22496 | 0.01 | 0.02 | 0.26 | 0.26 | 0.24 | 0.92 | 0.18 |
| ISAS - Mooring | 6789188 | 0.00 | 0.01 | 0.25 | 0.25 | 0.24 | 0.93 | 0.18 |
| Mercator - Mooring | 6799748 | -0.01 | -0.02 | 0.23 | 0.23 | 0.18 | 0.94 | 0.14 |
| ISAS - Mercator | 16365080 | 0.01 | 0.03 | 0.26 | 0.26 | 0.24 | 0.92 | 0.18 |

Numerical values of Table 1 can be downloaded as a csv file here.

# References

Alistair Adcroft, Chris Hill, and John Marshall. Representation of Topography by Shaved Cells in a Height Coordinate Ocean Model. *Mon. Weather Rev.*, 125(9):2293–2315, 1997. doi: 10.1175/1520-0493(1997)125⟨2293:ROTBSC⟩2.0.CO;2.

C. Amante and B. W. Eakins. ETOPO1 1 Arc-Minute Global Relief Model: Procedures, Data Sources and Analysis. Technical report, 2009.

Akio Arakawa and Vivian R. Lamb. A Potential Enstrophy and Energy Conserving Scheme for the Shallow Water Equations. *Mon. Weather Rev.*, 109(1):18–36, 1981. doi: 10.1175/1520-0493(1981)109⟨0018:APEAEC⟩2.0.CO;2.

J. J. Becker, D. T. Sandwell, W. H. F. Smith, J. Braud, B. Binder, J. Depner, D. Fabre, J. Factor, S. Ingalls, S-H. Kim, R. Ladner, K. Marks, S. Nelson, A. Pharaoh, R. Trimmer, J. Von Rosenberg, G. Wallace, and P. Weatherall. Global bathymetry and elevation data at 30 arc seconds resolution: Srtm30_plus. *Marine Geodesy*, 32(4):355–371, 2009. doi: 10.1080/01490410903297766.

Barnier Bernard, Gurvan Madec, Thierry Penduff, Jean-Marc Molines, Anne-Marie Treguier, Julien Le Sommer, Aike Beckmann, Arne Biastoch, Claus Böning, Joachim Dengg, Corine Derval, Edmée Durand, Sergei Gulev, Elizabeth Remy, Claude Talandier, Sébastien Theetten, Mathew Maltrud, Julie McClean, and Beverly De Cuevas. Impact of partial steps and momentum advection schemes in a global ocean circulation model at eddy-permitting resolution. *Ocean Dynam.*, 56(5):543–567, Dec 2006. ISSN 1616-7228. doi: 10.1007/s10236-006-0082-1.

Bruno Blanke and Pascale Delecluse. Variability of the tropical atlantic ocean simulated by a general circulation model with two different mixed-layer physics. *J. Phys. Oceanogr.*, 23(7): 1363–1388, 1993. doi: 10.1175/1520-0485(1993)023⟨1363:VOTTAO⟩2.0.CO;2.

Jaqueline Boutin, Y. Chao, W. E. Asher, T. Delcroix, R. Drucker, K. Drushka, N. Kolodziejczyk, T. Lee, N. Reul, G. Reverdin, J. Schanze, A. Soloviev, L. Yu, J. Anderson, L. Brucker, E. Dinnat, A. S. Garcia, W. L. Jones, C. Maes, T. Meissner, W. Tang, N. Vinogradova, and B. Ward. Satellite and In Situ Salinity: Understanding Near-Surface Stratification and Sub-footprint Variability. *Bull. Am. Meterol. Soc.*, 97(8):1391–1407, 2016. ISSN 1520-0477. doi: 10.1175/bams-d-15-00032.1.

Sophie Cravatte, Gurvan Madec, Takeshi Izumo, Christophe Menkes, and Alexandra Bozec. Progress in the 3-d circulation of the eastern equatorial pacific in a climate ocean model. *Ocean Modelling*, 17(1):28–48, 2007. ISSN 1463-5003. doi: https://doi.org/10.1016/j.ocemod.2006.11.003.

James A. Cummings. Operational multivariate ocean data assimilation. *Q. J. Roy. Meteor. Soc.*, 131(613):3583–3604, oct 2005. doi: 10.1256/qj.05.105.

James A. Cummings and Ole Martin Smedstad. *Variational Data Assimilation for the Global Ocean*, pages 303–343. Springer Berlin Heidelberg, 2013. ISBN 978-3-642-35088-7. doi: 10.1007/978-3-642-35088-7_13.

R. Droghei, B. Buongiorno Nardelli, and R. Santoleri. Combining In Situ and Satellite Observations to Retrieve Salinity and Density at the Ocean Surface. *J. Atmos. Oceanic Technol.*, 33 (6):1211–1223, jun 2016. doi: 10.1175/jtech-d-15-0194.1.

Riccardo Droghei, Bruno Buongiorno Nardelli, and Rosalia Santoleri. A New Global Sea Surface Salinity and Density Dataset From Multivariate Observations (1993–2016). *Frontiers in Marine Science*, 5, mar 2018. doi: 10.3389/fmars.2018.00084.

T. Fichefet and M. A. M. Maqueda. Sensitivity of a global sea ice model to the treatment of ice thermodynamics and dynamics. *J. Geophys. Res.*, 102(C6):12609–12646, 1997. doi: 10.1029/97JC00480.

G. Forget, J.-M. Campin, P. Heimbach, C. N. Hill, R. M. Ponte, and C. Wunsch. ECCO version 4: an integrated framework for non-linear inverse modeling and global ocean state estimation. *Geoscientific Model Development*, 8(10):3071–3104, oct 2015a. doi: 10.5194/gmd-8-3071-2015.

G. Forget, D. Ferreira, and X. Liang. On the observability of turbulent transport rates by argo: supporting evidence from an inversion experiment. *Ocean Sci.*, 11:839–853, 2015b. ISSN 1812-0792. doi: 10.5194/os-11-839-2015.

Gaël Forget and Rui M. Ponte. The partition of regional sea level variability. *Prog. Oceanogr.*, 137:173–195, 2015. ISSN 0079-6611. doi: 10.1016/j.pocean.2015.06.002.

D. N. Fox, W. J. Teague, C. N. Barron, M. R. Carnes, and C. M. Lee. The Modular Ocean Data Assimilation System (MODAS). *J. Atmos. Oceanic Technol.*, 19(2):240–252, feb 2002. doi: 10.1175/1520-0426(2002)019⟨0240:tmodas⟩2.0.co;2.

Fabienne Gaillard, Thierry Reynaud, Virginie Thierry, Nicolas Kolodziejczyk, and Karina von Schuckmann. In Situ-Based Reanalysis of the Global Ocean Temperature and Salinity with ISAS: Variability of the Heat Content and Steric Height. *J. Clim.*, 29(4):1305–1323, February 2016. ISSN 1520-0442. doi: 10.1175/jcli-d-15-0028.1.

E. C. Hunke and J. K. Dukowicz. An elastic–viscous–plastic model for sea ice dynamics. *J. Phys. Oceanogr.*, 27(9):1849–1867, 1997. doi: 10.1175/1520-0485(1997)027⟨1849:AEVPMF⟩2.0.CO;2.

Nicolas Kolodziejczyk, Gilles Reverdin, and Alban Lazar. Interannual Variability of the Mixed Layer Winter Convection and Spice Injection in the Eastern Subtropical North Atlantic. *J. Phys. Oceanogr.*, 45(2):504–525, Feb 2015. ISSN 1520-0485. doi: 10.1175/jpo-d-14-0042.1.

G. Madec. *NEMO ocean engine.* Note du Pôle de modélisation, Institut Pierre-Simon Laplace (IPSL), France, No 27, ISSN No 1288-1619, 2008.

Gurvan Madec and Maurice Imbard. A global ocean mesh to overcome the North Pole singularity. *Clim. Dyn.*, 12(6):381–388, May 1996. ISSN 1432-0894. doi: 10.1007/BF00211684.

John Marshall, Alistair Adcroft, Chris Hill, Lev Perelman, and Curt Heisey. A finite-volume, incompressible navier stokes model for studies of the ocean on parallel computers. *J. Geophys. Res.*, 102:5753–5766, 1997. ISSN 0148-0227. doi: 10.1029/96jc02775.

B. Buongiorno Nardelli, R. Droghei, and R. Santoleri. Multi-dimensional interpolation of SMOS sea surface salinity with surface temperature and in situ salinity data. *Remote Sens. Environ.*, 180:392–402, jul 2016. doi: 10.1016/j.rse.2015.12.052.

G. Roullet and G. Madec. Salt conservation, free surface, and varying levels: A new formulation for ocean general circulation models. *J. Geophys. Res.*, 105(C10):23927–23942, 2000. doi: 10.1029/2000JC900089.

Anthony Weaver and Philippe Courtier. Correlation modelling on the sphere using a generalized diffusion equation. *Q. J. Roy. Meteor. Soc.*, 127(575):1815–1846, July 2001. ISSN 1477-870X. doi: 10.1002/qj.49712757518.

Carl Wunsch and Patrick Heimbach. Chapter 21 - dynamically and kinematically consistent global ocean circulation and ice state estimates. In Gerold Siedler, Stephen M. Griffies, John Gould, and John A. Church, editors, *Ocean Circulation and Climate*, volume 103 of *International Geophysics*, pages 553–579. Academic Press, 2013. doi: https://doi.org/10.1016/B978-0-12-391851-2.00021-0.

Carl Wunsch, Patrick Heimbach, Rui Ponte, and Ichiro Fukumori. The Global General Circulation of the Ocean Estimated by the ECCO-Consortium. *Oceanography*, 22(2):88–103, 2009. ISSN 1042-8275. doi: 10.5670/oceanog.2009.41.